

## Full Length Research Article

### A MODEL FOR THE FLOW OF NATURAL GAS THROUGH A PIPELINE IN TWO-DIMENSIONAL CYLINDRICAL COORDINATES

<sup>1</sup>Effiong, E.E., <sup>1</sup>Orga, A.C., <sup>1</sup>Ibe, E.C., \*<sup>1</sup>Ekeke I. C. and <sup>2</sup>Nzebuka, C. G.

<sup>1</sup>Chemical Engineering Department Federal University of Technology, Owerri, Imo State, Nigeria

<sup>2</sup>Materials and Metallurgical Engineering Department Federal University of Technology, Owerri, Imo State, Nigeria

Accepted 29<sup>th</sup> October, 2016; Published Online 30<sup>th</sup> November, 2016

#### ABSTRACT

A model for predicting flow properties in a natural gas pipeline is presented in this paper. The method involves a two-dimensional gas pipeline model in axisymmetric cylindrical coordinates. The flow is assumed compressible and steady. Steady compressible natural gas flow through a pipeline was studied by the use of a finite volume method. First, the standard  $k-\epsilon$  turbulence equations were modeled together with the Navier Stokes System of equations via the Reynolds-Averaged method. The Soave-Redlich-Kwong equation of state was also included as an auxiliary equation. Finally the Pressure Implicit with Splitting of Operators (PISO) applied on a staggered grid was used as method of solution. Computer simulation was then carried out to determine pressure, density, velocity, temperature, eddy viscosity, turbulence eddy dissipation and turbulence kinetic energy variation within the pipeline system. Parametric analysis was also carried out.

**Key words:** Compressible flow; Finite volume; Cylindrical; Navier-Stokes; Turbulence; Natural gas.

#### INTRODUCTION

A gas distribution network is composed of pipe segments connected by simple junctions or other components (compressor stations, pressure regulators, valves, etc.), (Luongo, Cesar, a, (1986). The mass of gas flowing through each of these components at any given time is negligible compared with the gas contained in the pipe segments. This assumption allows only a quasi-steady state treatment of these components and leaves the pipe sections as the only distributed system requiring the solution of partial differential equations for its characterization. Gas flow in pipelines can be steady or unsteady. Steady gas flow presents little or no problems unlike unsteady gas flow. Unsteady gas flow in pipelines occurs due to rapid and slow disturbances (Nouri-Borujerdi, 2011). In general, pressure and mass-flow fluctuations cause slow disturbances whereas rapid disturbances are associated with compression wave effects caused by sharp closure of a shut-off valve, the system startup or expansion wave related to the pipeline rupture. The unsteady flow of gas in a long pipeline after an accidental rupture is of considerable interest to the natural gas industry due to the enormous amount of flammable gas release and its potential hazards. The accurate prediction of outflow and its variation with time following pipeline rupture or (any other

disturbance in the system) are therefore extremely important since this information dictates all the major consequences associated with such failure including fire, system shut down, explosion and environmental pollution (Mahgerefteh *et al*, 2006. However, under certain assumptions, flow through a pipeline can considered steady. Costa *et al*. (1998) presented a model and an algorithm for the one-dimensional steady state simulation of any pipeline network configuration with compressible fluids. The model can predict pressures, flow rates, temperatures and gas compositions at any point of the network. This model is made up of a system of algebraic linear and nonlinear equations. The model was solved using the Newton-Raphson Method associated with a successive substitution procedure. The potential of the simulator is explored by the analysis of a pressure relief network, using a stochastic procedure for the evaluation of system performance. Zogheib (2010) presented a new numerical method for solving the two-dimensional, steady, incompressible viscous flow equations on a curvilinear staggered grid. The proposed methodology is finite difference based, but essentially takes advantage of the best features of both the finite difference and finite volume methods. Gupta and Kalita (2005) proposed a new method for solving Navier–Stokes equations. The proposed methodology is based on a stream function–velocity formulation of the two-dimensional steady-state Navier–Stokes equations representing incompressible fluid flows in two-dimensional domains. Venturin *et al*. (2010) numerically obtained a steady state solution of the evolution

\*Corresponding author: Ekeke I. C.

Chemical Engineering Department Federal University of Technology, Owerri, Imo State, Nigeria

incompressible and the compressible Navier-Stokes equations by the Characteristic Based Split Scheme accelerated with the Minimum Polynomial Extrapolation Scheme. The developed algorithm was tested on two-dimensional benchmark problems. It demonstrates the new computational features arising from the introduction of the extrapolation procedure in the CBS scheme. The results showed a remarkable reduction of the computational cost of the simulations. Kolluru *et al* (2012) carried out a numerical study of aerodynamic characteristics in steady laminar supersonic flow over a double wedge airfoil using finite element based CFD software tool "ComsolMultiphysics". The aerodynamic characteristics namely; lift and drag were analysed by numerically solving compressible Navier-Stokes equations in the flow field around double wedge airfoil by parameterising the angle of attack  $\alpha$  and thickness to chord ratio. Hassan *et al* (1991) presented a fast algorithm for constructing continuous lines, made up of element sides, which pass once through each node of a general unstructured triangular mesh and which are generally aligned in prescribed directions. The lines were employed as the basis of an adaptive fully implicit unstructured grid procedure for the solution of two-dimensional problems of steady compressible inviscid and laminar viscous high-speed flows, where the equation system was solved by line relaxation using a block tridiagonal equation solver. Noorbehesht (2012), modeled natural gas flow in a transmission line at steady state in 2D cylindrical coordinates. The Navier Stokes equation, the ideal gas equation and the k- $\epsilon$  turbulence models were applied. A finite volume method was then used for the solution of the equations. Results obtained by this method agreed very well with experimental data obtained from the National Iranian Gas Company. This work presents a model for the simulation of steady compressible flow of natural gas through a pipeline in 2-dimensional axisymmetric cylindrical coordinates. The Navier-Stokes system of equations, the energy equation and the k  $\epsilon$  turbulence equation were the basic equations employed. The Soave-Redlich Kwong equation of state was used as an auxiliary equation. A finite volume method of solution used to solve the resulting set of equations is also presented. To the authors' knowledge, no such method of solution has been published for the model in question considered. Variation of certain flow variables along the pipeline is presented as well. Parametric analyses are also being illustrated.

## Nomenclature

$V_r$ , velocity in the radial (r) direction, m/s  
 $V_z$ , velocity in the axial (z) direction, m/s  
 $V_\theta$ , velocity in the azimuthal direction  
 $V$ , volume  
 $R$ , radial direction, m  
 $x$ , axial direction, m  
 $T$ , temperature, K  
 $T_c$ , critical temperature, K  
 $E$ , total internal energy, J  
 $k$ , thermal conductivity, W/m.K  
 $k$ , kinetic energy of turbulence, J/Kg  
 $P$ , pressure, N/m<sup>2</sup>  
 $P_c$ , critical pressure, N/m<sup>2</sup>  
 $C_p$ , constant pressure specific heat capacity, J/KgK  
 $q$ , heat flux, W/m<sup>2</sup>  
 $R$ , gas constant, J/kg. K

$a, b, m$ , constants  
 $G_k$ , constant for turbulence kinetic energy,  
 $G_\epsilon$ , constant for specific dissipation rate,  
 $G_T$ , constant for specific dissipation rate,  
 $S$ , source term

## Greek Characters

$\mu$ , dynamic viscosity, Ns/m<sup>2</sup>  
 $\rho$ , density, kg/m<sup>3</sup>  
 $\tau$ , shear stress tensor, N/m<sup>2</sup>  
 $\epsilon$ , turbulence dissipation rate, m<sup>2</sup>/s<sup>3</sup>  
 $\theta$ , azimuthal direction  
 $\omega$ , centric factor

## Subscripts

$E, e$ , East  
 $N, n$ , North  
 $S, s$ , South  
 $W, w$ , West  
 $t$ , turbulence

## The Model equations

The basic equations used to model flow in pipelines at steady state and employed in this work are the Navier-Stokes equations presented below.

## Assumptions

The cross-sectional area of the pipe is constant.  
 The gas flow is highly turbulent.

## Conservation of mass or continuity equation (Bird *et al*, 2002);

$$\frac{1}{r} \frac{\partial}{\partial r} (\rho r V_r) + \frac{\partial}{\partial z} (\rho V_z) = 0 \quad (1)$$

## Conservation of Momentum equation in terms of $\tau$ in the r-directions (Bird *et al*, 2002);

$$\frac{1}{r} \frac{\partial (r \rho V_r V_r)}{\partial r} + \frac{\partial (\rho V_r V_z)}{\partial z} = -\frac{\partial P}{\partial r} - \frac{1}{r} \frac{\partial}{\partial r} (r \tau_{rr}) - \frac{\partial}{\partial z} \tau_{zr} + \frac{\tau_{\theta\theta}}{r} \quad (2)$$

## Conservation of Momentum equation in terms of $\tau$ in the z-directions (Bird *et al*, 2002);

$$\frac{1}{r} \frac{\partial (r \rho V_r V_x)}{\partial r} + \frac{\partial (\rho V_z V_z)}{\partial z} = \frac{\partial P}{\partial r} - \frac{1}{r} \frac{\partial}{\partial r} (r \tau_{zr}) - \frac{\partial}{\partial z} \tau_{zz} \quad (3)$$

where

$$\tau_{rr} = \mu_{eff} \left( 2 \frac{\partial V_r}{\partial r} - \frac{2}{3} (\nabla \cdot v) \right) \quad (4)$$

$$\tau_{xz} = \mu_{eff} \left( 2 \frac{\partial V_z}{\partial z} - \frac{2}{3} (\nabla \cdot v) \right) \quad (5)$$

$$\tau_{xr} = \mu_{eff} \left( \frac{\partial V_r}{\partial z} + \frac{\partial V_z}{\partial r} \right) \quad (6)$$

$$\tau_{\theta\theta} = \mu_{eff} \left( 2 \frac{V_r}{r} \frac{\partial}{\partial r} (r \cdot v) \right) \quad (7)$$

$$\nabla \cdot v = \frac{1}{r} \left( \frac{\partial}{\partial r} \right) (r V_r) + \frac{\partial V_z}{\partial z} \quad (8)$$

$\mu_{eff} = \mu + \mu_t = \text{effective viscosity}$  (Blazek, 2001, Noorbehesht, 2012)

### Conservation of Energy Equation

$$\begin{aligned} \frac{\partial}{\partial z} (\rho c_p V_z T) + \frac{1}{r} \frac{\partial}{\partial r} (r \rho c_p V_r T) \\ = \frac{\partial}{\partial z} \left( \left( \lambda + \frac{c_p \mu_t}{G_T} \right) \frac{\partial T}{\partial z} \right) \\ + \frac{1}{r} \frac{\partial}{\partial r} \left( r \left( \lambda + \frac{c_p \mu_t}{G_T} \right) \frac{\partial T}{\partial r} \right) + S_T \end{aligned} \quad (9)$$

### Equation of State

The equation of state adopted in this work is the Soave-Redlich-Kwong equation stated as follows ([https://www.education.psu.edu/png520/m10\\_p5.htm](https://www.education.psu.edu/png520/m10_p5.htm))

$$P = \frac{RT}{V - b} - \frac{a(T)}{V(V + b)} \quad (10)$$

$$w \text{ ere } a(T) = 0.4274 \left( \frac{R^2 T_c^2}{P_c} \right) \left\{ 1 + m \left[ 1 - \left( \frac{T}{T_c} \right)^{0.5} \right] \right\}^2 \quad (11)$$

$$m = 0.480 + 1.57\omega - 0.176\omega^2 \quad (12)$$

$$b = 0.08664 \frac{RT_c}{P_c} \quad (13)$$

### Turbulence Kinetic Energy

$$\begin{aligned} \frac{\partial}{\partial x} (\rho V_x k) + \frac{1}{r} \frac{\partial}{\partial r} (r \rho V_r k) \\ = \frac{\partial}{\partial x} \left( \left( \mu + \frac{\mu_t}{G_k} \right) \frac{\partial k}{\partial x} \right) \\ + \frac{1}{r} \frac{\partial}{\partial r} \left( r \left( \mu + \frac{\mu_t}{G_k} \right) \frac{\partial k}{\partial r} \right) + S_k \end{aligned} \quad (14)$$

### Turbulence Dissipation Rate

$$\begin{aligned} \frac{\partial}{\partial x} (\rho V_x \varepsilon) + \frac{1}{r} \frac{\partial}{\partial r} (r \rho V_r \varepsilon) \\ = \frac{\partial}{\partial x} \left( \left( \mu + \frac{\mu_t}{G_\varepsilon} \right) \frac{\partial \varepsilon}{\partial x} \right) \\ + \frac{1}{r} \frac{\partial}{\partial r} \left( r \left( \mu + \frac{\mu_t}{G_\varepsilon} \right) \frac{\partial \varepsilon}{\partial r} \right) + S_\varepsilon \end{aligned} \quad (15)$$

Where  $S_k = \mu_t g$ ,  $\rho \varepsilon$ ,  $S_\varepsilon = C_1 g \mu_t \varepsilon k$ ,  $C_2 \rho \frac{\varepsilon^2}{k}$  and

$$\mu_t = C_\mu \rho \frac{k^2}{\varepsilon}$$

$C_\mu = 0.09$ ,  $C_1 = 1.4$ ,  $C_2 = 1.92$ ,  $G_k = 1.00$ ,  $G_\varepsilon = 1.3$ ,  $G_T = 0.85$ .

### Numerical Technique

The finite volume method is the numerical solution method of choice adopted in this work. In employing the use of the finite volume method, the general form of the conservation equations of fluid for the geometry considered in this work, for any scalar variable  $\phi$  can be represented as follows

$$\begin{aligned} \frac{\partial}{\partial x} (\rho V_x \phi) + \frac{1}{r} \frac{\partial}{\partial r} (r \rho V_r \phi) \\ = \frac{\partial}{\partial x} \left( \Gamma \frac{\partial \phi}{\partial x} \right) + \frac{1}{r} \frac{\partial}{\partial r} \left( r \Gamma \frac{\partial \phi}{\partial r} \right) + S_\phi \end{aligned} \quad (16)$$

$\phi$  represents any of the variables,  $V_r, V_x, T, k$  and  $\varepsilon$  while  $\Gamma$  represents  $\mu$  and  $k$ . In employing the method, bracketed smaller contributions to the viscous stress terms in the transport equation are hidden (Versteeg and Malalasekera, 2007). Equations 1, 2, 3, 10, 15 and 16 are then integrated over a control volume after which Gauss' divergence theorem is applied to give the following;

$$\begin{aligned} \int_A n \cdot (\rho V_x \phi) dA + \int_A n \cdot (r \rho V_r \phi) dA \\ = \int_A n \cdot \left( \Gamma \frac{\partial \phi}{\partial x} \right) dA + \int_A n \cdot \left( r \Gamma \frac{\partial \phi}{\partial r} \right) dA \\ + \int_{CV} S_\phi dV \end{aligned} \quad (17)$$

The solution region comprising of a grid is then divided into discrete control volumes (CV). The CV surface consists of four (in 2D) plane faces, denoted by lower-case letters corresponding to their direction (e, w, n, s) with respect to the central node (P) (Ferziger and Peric, 2012). The governing equations are then integrated over the CV to obtain a discrete equation on node P. The equation is as follows;

$$\begin{aligned} (\rho V_x A \phi)_e - (\rho V_x A \phi)_w + (\rho V_r A \phi)_n - (\rho V_r A \phi)_s \\ = \left( \Gamma A \frac{\partial \phi}{\partial x} \right)_e - \left( \Gamma A \frac{\partial \phi}{\partial x} \right)_w + \left( \Gamma A \frac{\partial \phi}{\partial r} \right)_n \\ - \left( \Gamma A \frac{\partial \phi}{\partial r} \right)_s + (S_p \phi_p + S_u) V_p \end{aligned} \quad (18)$$

The integration of the continuity equation also gives;

$$(\rho V_x A)_e - (\rho V_x A)_w + (\rho V_r A)_n - (\rho V_r A)_s = 0 \quad (19)$$

In the discretization of the governing equations, central differencing scheme is used for the spatial diffusion terms and upwind differencing scheme in the spatial convection terms. The general discrete equation is then;

$$a_p \phi_p = a_w \phi_w + a_e \phi_e + a_s \phi_s + a_n \phi_n + S_U \quad (20)$$

Where  $a_p = a_w + a_e + a_s + a_n + Fr - S_p$ ,

$$Fr = (F_e r - F_w r) + (F_n r - F_s r)$$

$$F_e = (\rho U)_e A_e, \quad F_w = (\rho U)_w A_w, \quad F_n = (\rho U)_n A_n, \quad F_s = (\rho U)_s A_s$$

Next, the staggered arrangements have to be used as shown in figure 1 below. Since the momentum equations are coupled with pressure term, a method developed by Issa (1986) is employed in the computations. This method is called Pressure-Implicit with Splitting of Operators (PISO). The method is an improvement to Semi-Implicit-Pressure Link Equation (SIMPLE) algorithm originally invented by Patankar and

Spalding (1972). It is essentially a guess-and-correct procedure (Versteeg and Malalasekera, 2007) for the calculation of pressure on the staggered grid. The idea of using staggered grid arrangement developed by Harlow and Welch (1965) and adopted for this work from Versteeg and Malalasekera (2007) is to evaluate scalar variables, such as pressure, density, temperature, turbulence kinetic energy and dissipation rate at ordinary nodal points ( $\bullet$ ) where they are stored, and to calculate velocity components on staggered grids centered around the cell faces of scalar control volume. Horizontal arrows ( $\rightarrow$ ) indicate locations for  $u$ -control volume and vertical arrows ( $\uparrow$ ) denote those for  $v$ -control volumes. The reason for using staggered grid in solving pressure-velocity coupling equation is as a result of the fact that a uniform pressure field will be obtained if velocity and pressure were stored at the same nodal points.

### Boundary conditions

The boundary conditions for gas flow in pipeline in a 2D geometry are as shown in Figure 2

### Steady state condition

Fluid boundaries:

- Inlet:  $P$ ,  $u$ ,  $T$  are defined and  $\rho$  is defined by state equation.
- Outlet: general condition of fluid which is almost commonly applied in finite volume methods as follows (Versteeg and Malalasekera, 1995; Noorbehesht, 2012):

$$\frac{\partial T}{\partial n} = 0 \text{ and } \frac{\partial u_n}{\partial n} = 0$$

And a defined  $P_{out}$  aiming considered mass flow rate, and  $n$  is the normal outward vector of outlet surface.

Solid boundary:

No slip condition;  $u = u_w = 0$

Constant temperature on the wall;  $T = T_w$

Symmetric boundary condition;  $\frac{\partial \phi}{\partial n} = 0$

### Operating Conditions

Pipe diameter  $D = 0.35\text{m}$ , pipeline length  $L = 500\text{m}$ ; inlet pressure  $P_{in} = 26337.01\text{Pa}$ ; outlet pressure  $P_{out} = 20574.05\text{Pa}$ ; inlet temperature  $T_{in} = 46.86\text{ }^\circ\text{C}$ ; outlet temperature  $T_{out} = 34\text{ }^\circ\text{C}$ ; Physical properties of gas; the current properties of the gas are assumed constant. Molecular weight  $M_w = 19$ ; thermal conductivity  $k = 0.0332\text{ W/m.k}$ ; specific heat at constant pressure  $C_p = 2530\text{ J/kg.k}$ ; viscosity,  $\mu = 1.56 \times 10^{-5}\text{ kg/m.s}$ ;

### Model Validation

To validate the model, pressure data published by Noorbehesht (2012) which he obtained from the National Iranian Gas Company for the validation of a model he proposed were used. The pipeline he considered for simulation was 135Km in length. For the purpose of validation of the model considered in this work, this pipeline was scaled down to 500m. The inlet and outlet pressures were then scaled down to obtain an accurate result for the pressure profile. The profile is similar to that obtained by Noorbehesht. This proves the accuracy of the solution used for the model. Profiles for temperature, density, velocity, eddy viscosity, turbulence dissipation and turbulence kinetic energy along the pipeline were also obtained.

## RESULTS

The following graphical results were obtained after the simulation.

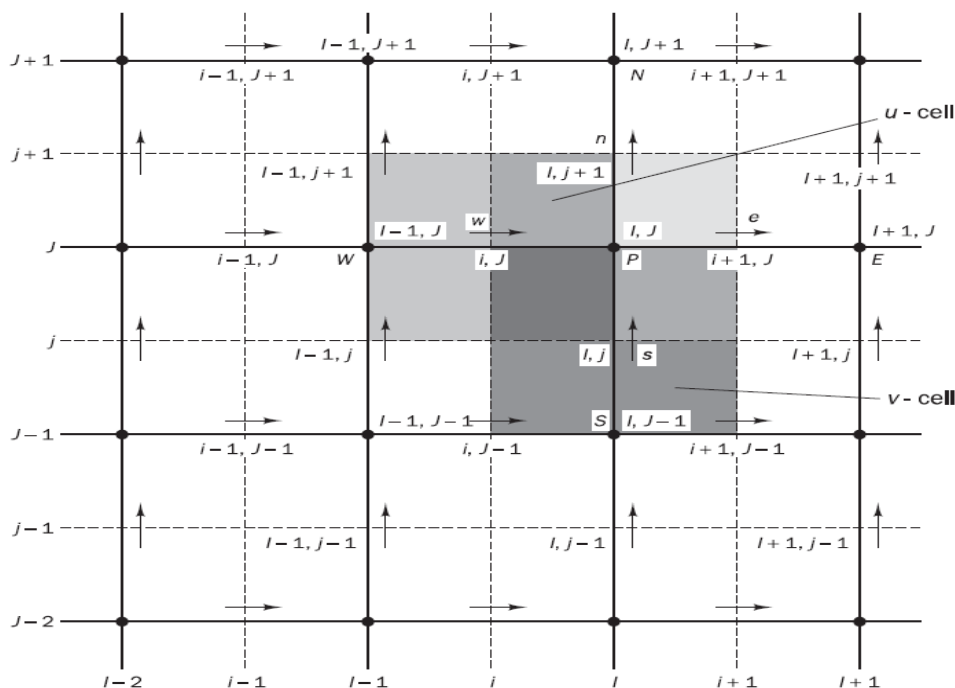


Figure 1. Staggered Structured Grid Arrangement for Pressure and Velocity

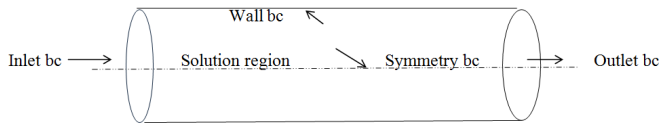


Figure 2. Flow domain and boundary conditions (Noorbehesht, 2012)

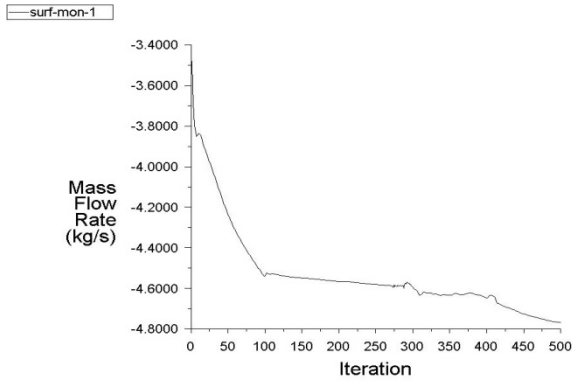


Figure 3. Plot of mass flow rate against number of iterations

Table 1. Mass Balance

Mass Flow Rate	(kg/s)
inlet	4.7635317
outlet	-4.766964
Net	-0.0034322739

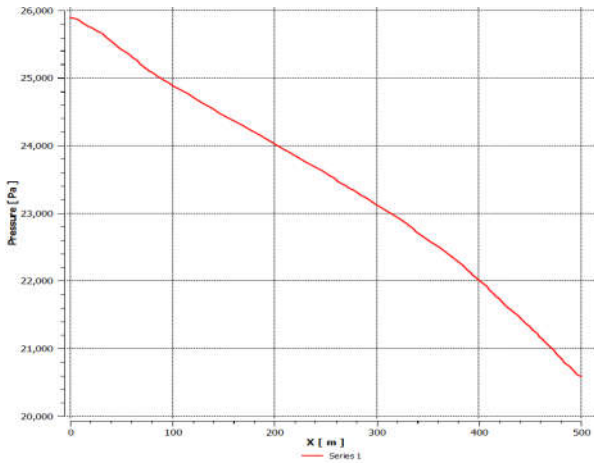


Figure 4. Graph of pressure distribution along the length of the pipeline

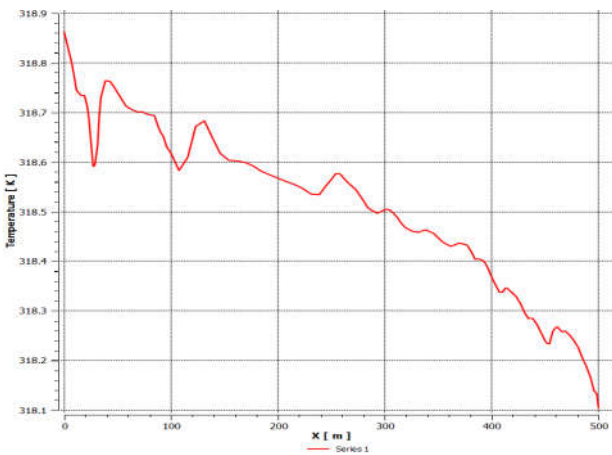


Figure 5. Graph of temperature distribution along the length of the pipeline

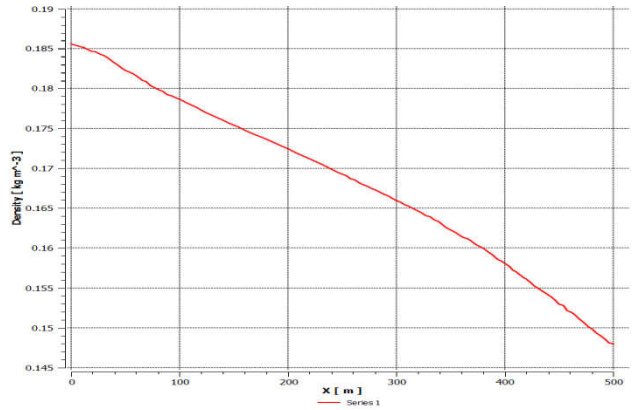


Figure 6. Density distribution along the length of the pipeline

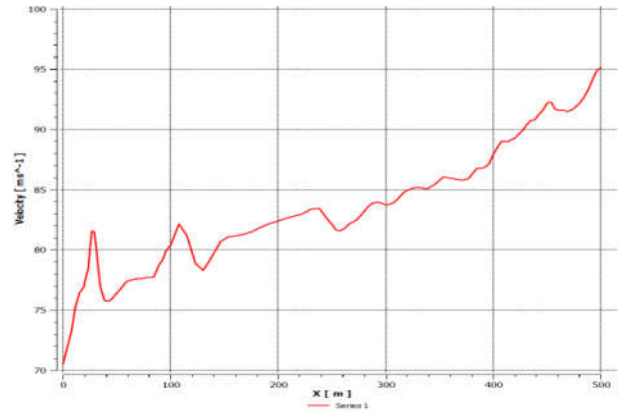


Figure 7. Velocity distribution along the length of the pipeline

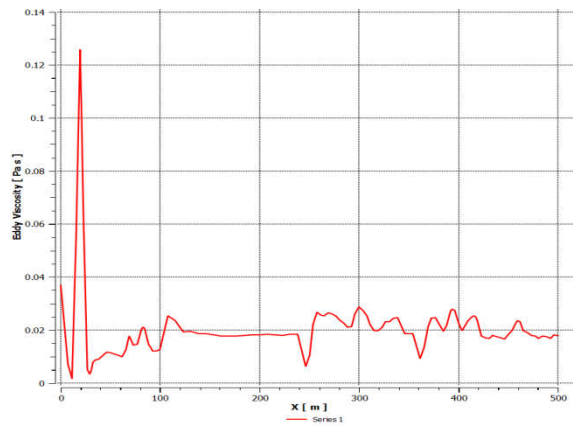


Figure 8. Steady state eddy viscosity distribution along the pipe

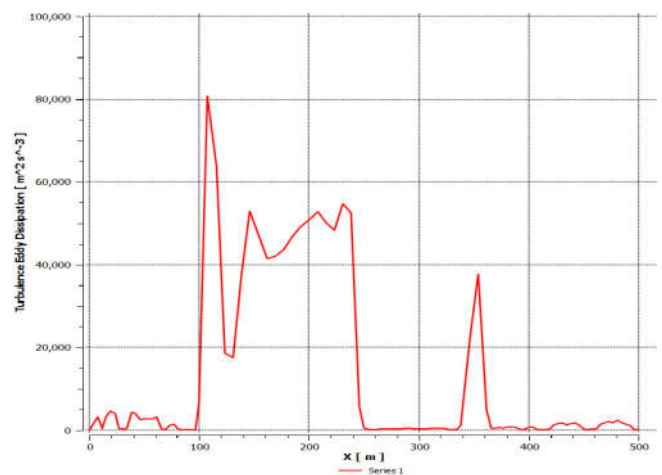


Figure 9 Steady state turbulence eddy dissipation distributions along the pipe

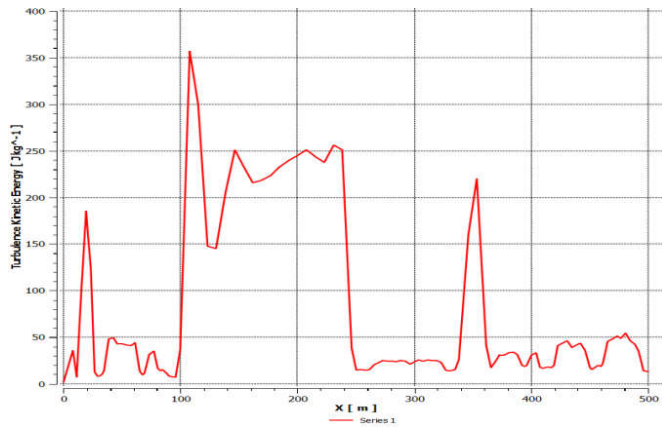


Figure 10. Steady state turbulence kinetic energy distributions along the pipe

above shows a graph of pressure variation along the pipe. The graph shows a drop in pressure from 25900Pa to 20,600Pa 500m downstream of the pipe.

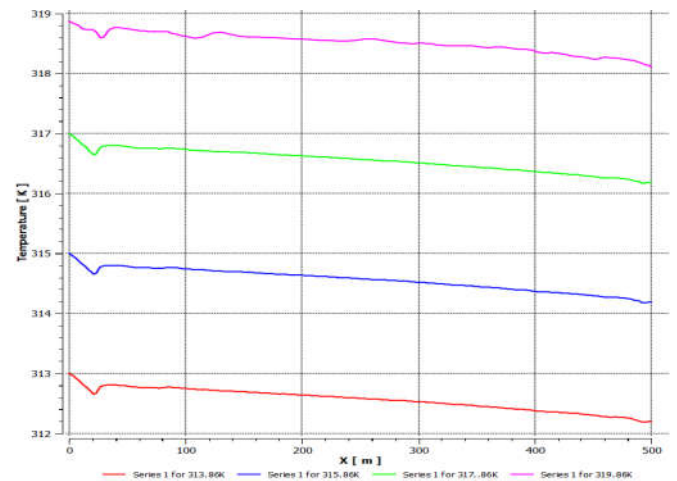


Figure 13. Gas flow temperature variations versus inlet temperature along the pipeline

**Parametric analysis:** Effect of inlet temperature on flow parameters

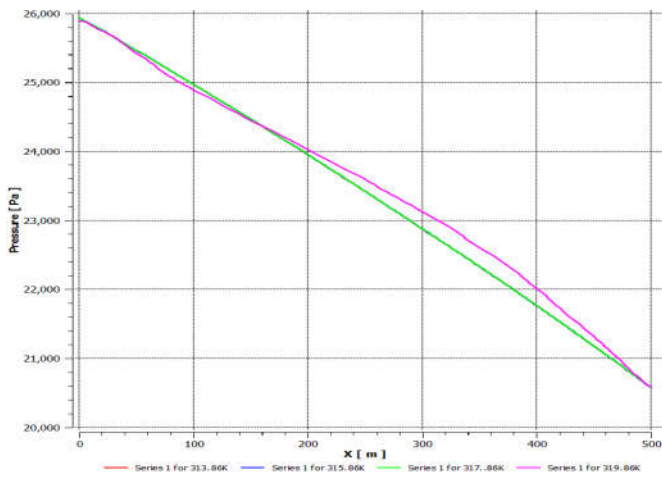


Figure 11. Gas flow pressure variations versus inlet temperature along the pipeline

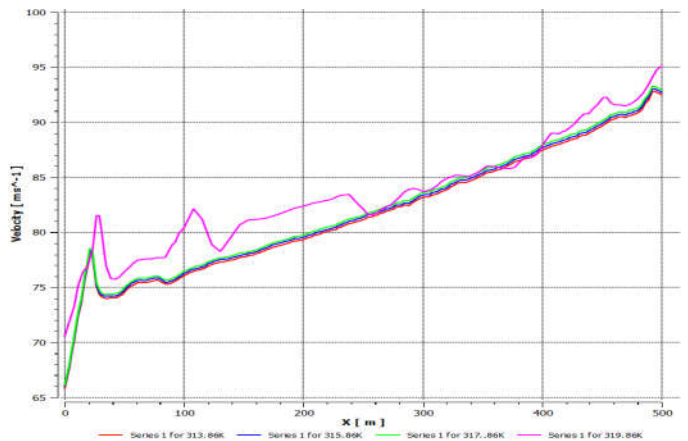


Figure 14. Gas flow velocity variations versus inlet temperature along the pipeline

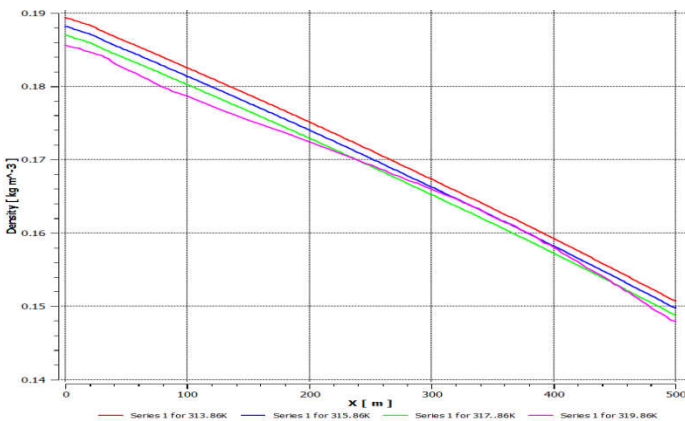


Figure 12. Gas flow density variations versus inlet temperature along the pipeline

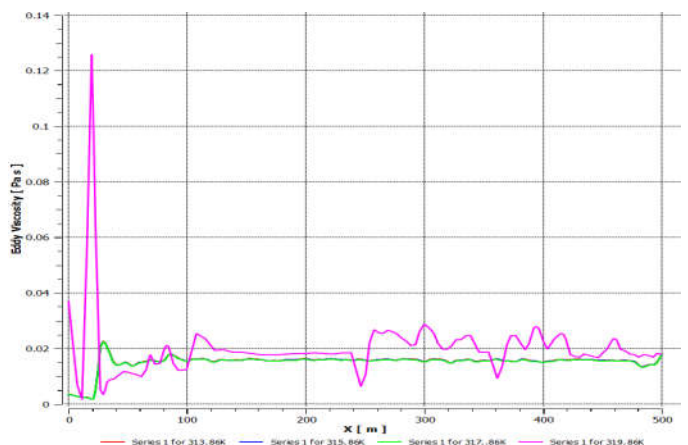


Figure 15. Gas flow eddy viscosity variations versus inlet temperature along the pipeline

**DISCUSSIONS**

The mass flow rate history in Figure 3 indicates that the solution has converged. Mass balance is also shown in Table 1. The net mass imbalance ideally should be a small fraction of the total flux through the system. The result therefore indicates that mass is being conserved in the system. Figure 4

This is to be expected since for a fluid flowing down a conduit, there's usually a pressure drop due to frictional resistance. The Figure 5 above shows a plot of temperature distribution in the pipe. There is also a decrease in its value as the gas flows down the pipe. Thus the trend is the same as that

of the pressure as can be seen since from the equation of state, pressure is directly proportional to temperature.

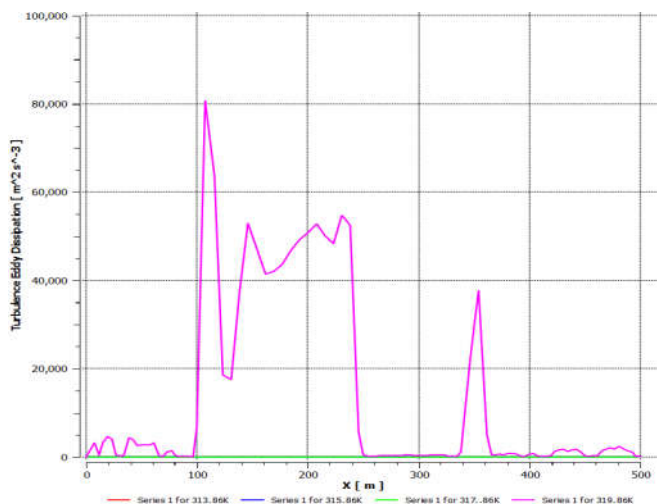


**Figure 16. Gas flow turbulence eddy dissipation variations versus inlet temperature along the pipeline**

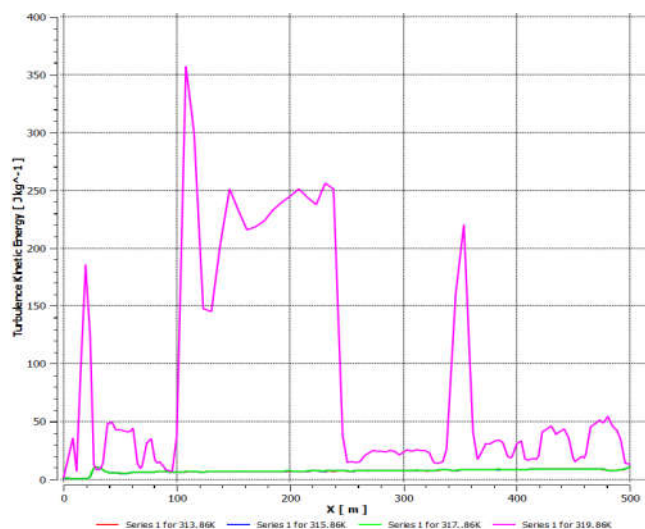


**Figure 17. Gas flow turbulence kinetic energy variations versus inlet temperature along the pipeline**

Figure 6 and figure 7 show plots of density and velocity respectively. It can be seen that density decreases along the length of the pipeline while the velocity plot shows a reverse trend. This is in agreement with the following equation (which shows that velocity increases with density decrease);

$$m = \rho uA \quad (21).$$

Eddy viscosity distributions along the pipe are illustrated in the figure 8 above. A fluctuation in the values of this variable can be seen. This is in agreement with the fact that turbulence is being experienced in the pipeline. The viscosity for instance for the steady state plot, first decreases gradually to a value of about 0.12Pas at a distance of about 20m from the pipeline entrance and then increases sharply to 0.004Pas about 10m away after which it continues to oscillate along the length of the pipeline. The plots for the turbulent eddy dissipation rate and turbulent kinetic energy distribution shown in figure 9 and figure 10 respectively also exhibit a similar trend. These graphs

illustrate the chaotic movements of the gas molecules in the turbulent region. Figure 11 shows pressure variation at four different inlet temperatures along the pipeline length. According to figure 12, from the entrance region of the pipe up till about the middle, density decreases due to increase in the temperature at a constant inlet pressure. This is buttressed by the equation of state where it is seen that density has an inverse relationship with temperature. The trend continues with the graph of density at 317.86K showing the lowest trend up till about 440m down the pipeline length after which it reverts back to the former trend till the end of the pipeline.

In figure 13, gas temperature variation gradient increases as inlet temperature increases. But on the overall as is expected there is temperature decrease along the pipeline length. Figure 14 shows variation of velocity of gas with inlet temperature along the pipeline. Inlet velocity increases due to inlet temperature increase. This of course stems from the fact that motion of gas molecules (hence their velocity) increases as temperature increases in a given system. The trend continues up to the end of the pipeline with the graph at 319.86K showing the highest trend. Figures 15, 16 and 17 show plots for variation of eddy viscosity, turbulence eddy dissipation and turbulence kinetic energy respectively with temperature along the pipeline length. As expected there are oscillations in the graphs owing to turbulence. It can also be seen that the highest peaks noticed in the plots are for the highest temperature, 319.86K. This confirms the fact that the higher the temperature, the more the kinetic energy attained by the gas molecules and hence more turbulence will be experienced by the molecules in the system.

## Conclusions

This work has demonstrated a method for predicting flow properties in a natural gas pipeline at steady state. The method involves the use of the PISO algorithm on a staggered grid for simulation. The basic model equations used are the Navier Stokes system of equations, the energy equation and the k- $\epsilon$  turbulence equations all in 2D axisymmetric cylindrical coordinates. The Soave-Redlich-Kwong equation of state was employed as an auxiliary equation. The method can be adapted by the Oil and Gas industries for the knowledge/control of pipeline system behavior.

## REFERENCES

- Bird, R. B., Stewart, W. E. and Lightfoot, E. N. 2002. *Transport Phenomena* (pp. 844-847). John Wiley and Sons, Inc.
- Blazek, J. 2001. *Computational Fluid Dynamics: Principles and Applications*. Elsevier.
- Costa, A.L.H., de Medeiros J.L. and Pessoa, F.L.P. 1998. Steady-State Modeling And Simulation Of Pipeline Networks For Compressible Fluids. *Braz. J. Chem. Eng.* vol. 15 n. 4 São Paulo Dec. 1998.
- Ferziger, J. H. and Peric, M. 2002. Ch. 4Computational Methods for Fluid Dynamics (page 72).Springer.3<sup>rd</sup> edition.
- Gupta, M. M. and Kalita, J. C. 2005. A new paradigm for solving Navier–Stokes equations: streamfunction–velocity formulation. *Journal of Computational Physics*, xxx: xxx–xxx.

- Harlow, F. H. and Welch, J. E. 1965. Numerical Calculation of Time-dependent Viscous Incompressible Flow of Fluid with Free Surface. *Phys. Fluids*, 8, 2182–2189.
- Issa, R. I. 1986. Solution of Implicitly Discretised Fluid Flow Equations by Operator-Splitting. *J. Comput. Phys.*, 62, 40–65.
- Kolluru, R. and Gopal, V. 2012. Numerical Study of Navier-Stokes Equations in Supersonic Flow over a Double Wedge Airfoil using Adaptive Grids. Excerpt from the *Proceedings of the 2012 COMSOL Conference* in Bangalore.
- Luchini, P. and Quadrio, M. 2006. A low-cost parallel implementation of direct numerical simulation of wall turbulence. *Journal of Computational Physics*, Volume 211: Issue 2, pp 551-571.
- Luongo, C. A. 1986. An Efficient Program for Transient Flow Simulation in Natural Gas Pipelines, PSIG Annual Meeting, New Orleans, Louisiana.
- Mahgerefteh, H., Oke, A. O. and Rykov, Y. 2006. Efficient numerical solution for highly transient flows. *Chemical Engineering Science*.
- Noorbehesht, N. 2012. Numerical Simulation of Natural Gas Flow in Transmission Lines through CFD Method Considering Effective Parameters. *J. Basic. Appl. Sci. Res.*, 2(8)7473-7487.
- Nouri-Borujerdi, A. 2011. Transient modeling of Gas Flow in Pipelines following catastrophic failure. *Mathematical and Computer Modeling*, 54: 3037–3045.
- Patankar, S. V. 1980. *Numerical Heat Transfer and Fluid Flow* Hemisphere Publishing Corporation, Taylor and Francis Group, New York.
- Venturin, M., Bertelle, R. and Russo, M. R. 2010. An accelerated algorithm for the Navier-Stokes equations. *Simulation Modelling Practice and Theory*, 18(2), 217-229.
- Versteeg, H K and W Malalasekera, W. 2007. *An introduction to computational fluid dynamicsthe finite volume method, second edition*. Longman Scientific and Technical. ([https://www.e-education.psu.edu/png520/m10\\_p5.htm](https://www.e-education.psu.edu/png520/m10_p5.htm))
- Versteeg, H. K. and Malalasekera, W. 1995. *An introduction to computational fluid dynamicsthe finite volume method, First edition*. Longman Scientific and Technical.

\*\*\*\*\*